JOURNAL OF SOLID STATE CHEMISTRY 56, 236–240 (1985)

High-Resolution Electron Microscopy of Defects in $W_4Nb_{26}O_{77}$

D. X. LI AND K. H. KUO

Institute of Metal Research, Academia Sinica, Shenyang, The People's Republic of China

Received February 15, 1984; in revised form July 13, 1984

Several different kinds of planar defects have been observed by means of high-resolution electron microscopy in $W_4Nb_{26}O_{77}$, such as disordered intergrowth of $WNb_{12}O_{33}$ and $W_3Nb_{14}O_{44}$ structural slabs, locally ordered intergrowth with a sequence of AABAAB, two separate microdomains of $WNb_{12}O_{33}$ and $W_3Nb_{14}O_{44}$ coexisting with $W_4Nb_{26}O_{77}$ and a complicated intergrowth of $W_4Nb_{26}O_{77}$, N–Nb_2O_5, $W_3Nb_{14}O_{44}$, and $Nb_{31}O_{77}F$ types of structure. © 1985 Academic Press, Inc.

Introduction

Structural images recorded with a high-resolution electron microscope can provide information of local structure at atomic resolution and therefore can be used to reveal different kinds of structural defects in crystals. During the last 10 years, the high-resolution electron microscopy technique has been applied with great success to the studies of some of the crystallographic shear structures (*1*), block structures (*2–5*) and tunnel structures (*6, 7*) of transition metal oxides and a number of new structures and different kinds of planar defects have been found. The present paper reports high-resolution electron microscopic observations, at the level of atomic resolution, of various kinds of structural defects in $W_4Nb_{26}O_{77}$.

The sample, having a nominal composition of $4WO_3 \cdot 13Nb_2O_5$, was sealed in platinum capsules, heated at 1250°C for 2 days and quenched into water. X-Ray analysis confirmed the presence of only $W_4Nb_{26}O_{77}$. The crystals were ground in an agate mortar and dispersed in methanol. Thin fragments of the crystals were collected on a holey carbon film supported on a copper grid. High-resolution observations were carried out at 200 kV using a JEM200CX electron microscope equipped with a high-resolution top-entry goniometer stage. High-resolution structural images were recorded at a magnification of 5.3–8.5 × 10^5 times, using an objective aperture corresponding to a radius of 0.36 $Å^{-1}$ in the diffraction pattern.

The simulated image calculations were performed using the multislice method with a program written by K. Ishizuka (*8*). The following parameters were used. Spherical aberration coefficient, 1.2 mm; slice thickness, 3.82 Å; the focus spread due to chromatic aberration, 30 Å; incident beam convergence, 0.4 mrad; and the number of diffracted beam included in the dynamical diffraction calculation, 4225. The images were computed for a range of thickness up to 25 slices over a defocus range of −500 to −800 Å. The computed image for a defocus

0022-4596/85 $3.00

of −600 Å and a specimen thickness of 8 slices agrees quite well with the observed image.

Results

The crystal structure of $W_4Nb_{26}O_{77}$ has been determined by single-crystal X-ray analysis (*9*). This ternary oxide is monoclinic (space group $C2$) and its unit cell dimensions are $a = 29.74$, $b = 3.824$, $c = 25.97$ Å, $\beta = 92.3°$. This oxide contains two kinds of octahedral block, namely (3 × 4) and (4 × 4). The blocks of the same sort join together forming a continuous slab. A is a slab of (3 × 4) blocks present in $WNb_{12}O_{33}$ and B that of (4 × 4) blocks in $W_3Nb_{14}O_{44}$. These slabs themselves are stacked in a sequence of ABAB . . . forming the structure of $W_4Nb_{26}O_{77}$.

In the structural images, tetragonal tunnels and the projection of rows of Nb (or W) atoms parallel to the [010] direction can be identified as bright and dark dots, respectively, and the neighboring Nb–Nb (or W) atoms, 1.9 Å apart in the [010] projection, is clearly resolved (see Fig. 3). Many crystals of $W_4Nb_{26}O_{77}$ investigated so far were rich in defects. At least four types of defect can be recognized. On the basis of a one-to-one correspondence between the structural image contrast and crystalline features, the structural details of these defects observed in the electron micrograph can be analyzed.

The most common defect is a disordered intergrowth of $WNb_{12}O_{33}$ and $W_3Nb_{14}O_{44}$ structural slabs caused possibly by the local fluctuations in composition. For example, one kind of stacking sequence is . . . $ABAB^+BBBBBB^+AB^+BBB^+ABAB^+AB^+BB^+AB^+BB^+A$ . . . , as shown in Fig. 1. These defects are two-dimensional planar defects parallel to the *ab* planes and can be regarded as a kind of stacking fault. The symbol (+) represents the position where a fault occurs.

The structural image in Fig. 2 shows, respectively, two separate microdomains of $WNb_{12}O_{33}$ and $W_3Nb_{14}O_{44}$ coexisting with $W_4Nb_{26}O_{77}$ in one crystal fragment. Allpress *et al.* (*10*) have investigated earlier the structure of $W_4Nb_{26}O_{77}$ with the lattice fringe imaging method and found that the faulted areas contain groups of fringes with constant spacing of 11 or 15 Å, respectively. They considered these zones as mi-

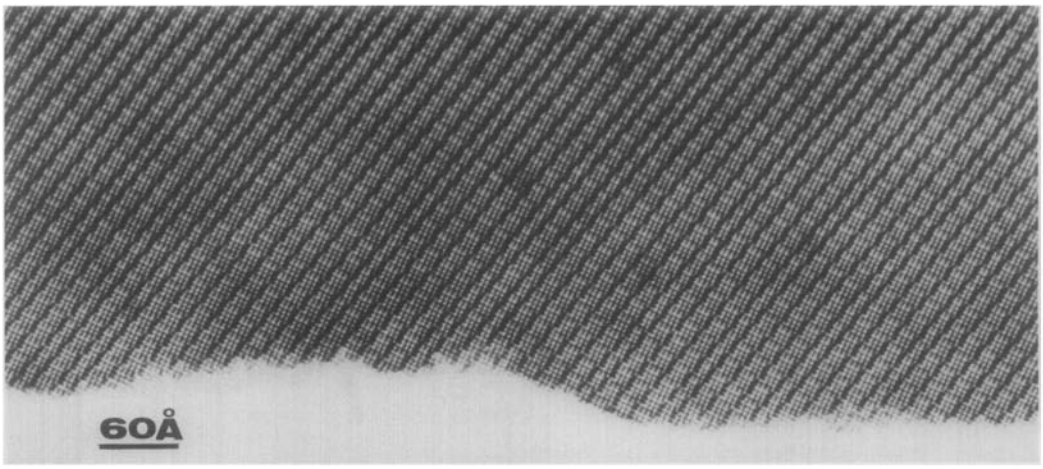

FIG. 1. Disordered intergrowth of $WNb_{12}O_{33}$ (A) and $W_3Nb_{14}O_{44}$ (B) structural slabs in a sequence of . . . ABABBBBBBABBBBABABBBBBABBBABBBAB . . . in [010] projection.

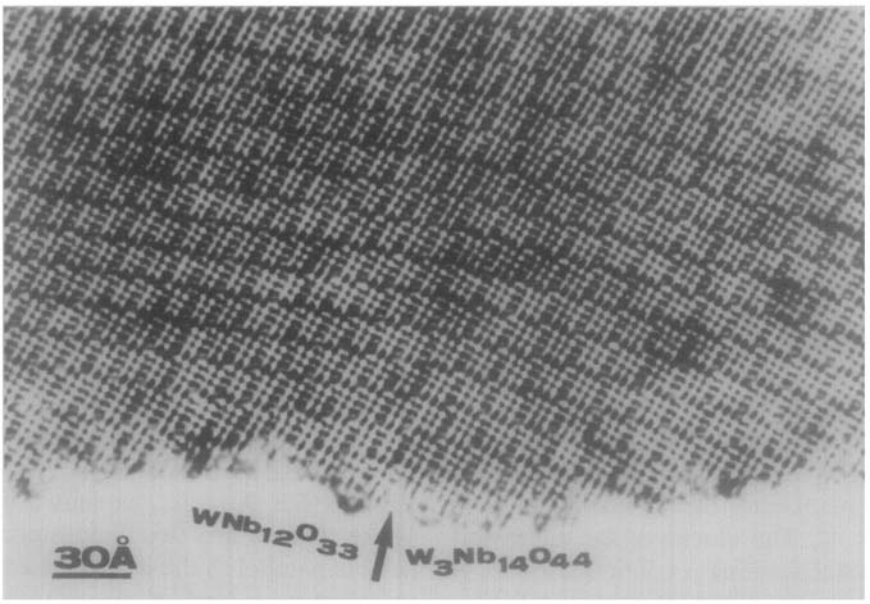

FIG. 2. Microdomains of the two phases $WNb_{12}O_{33}$ and $W_3Nb_{14}O_{44}$, coexisting with $W_4Nb_{26}O_{77}$ in [010] projection.

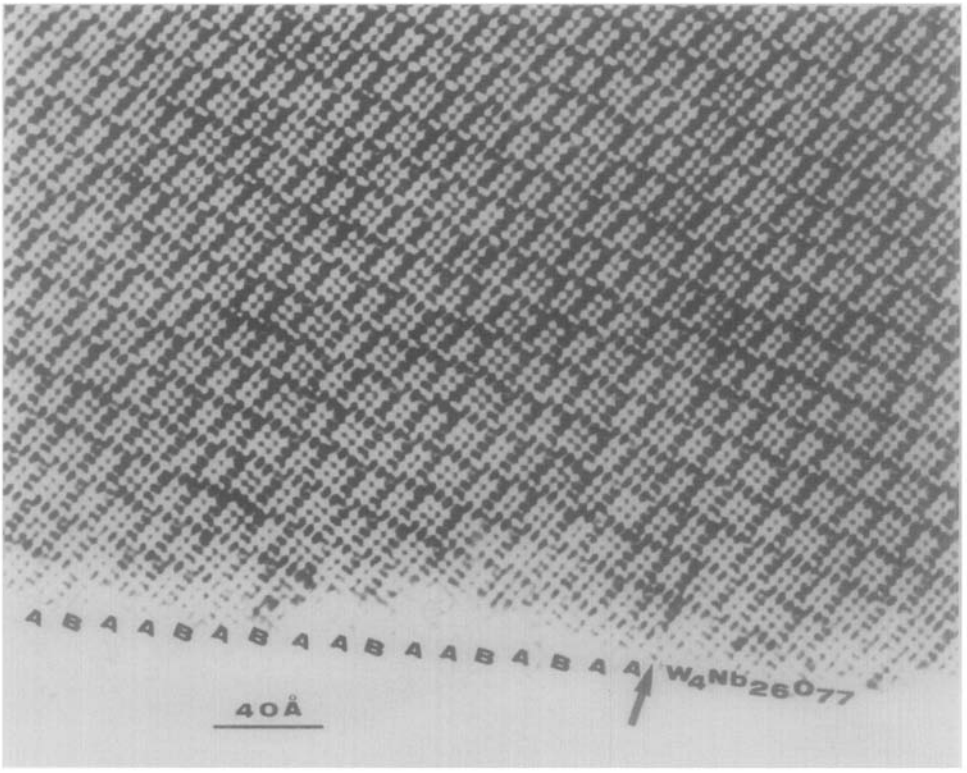

FIG. 3. The [010] structural image of an ordered intergrowth with a local sequence of AABAAB.

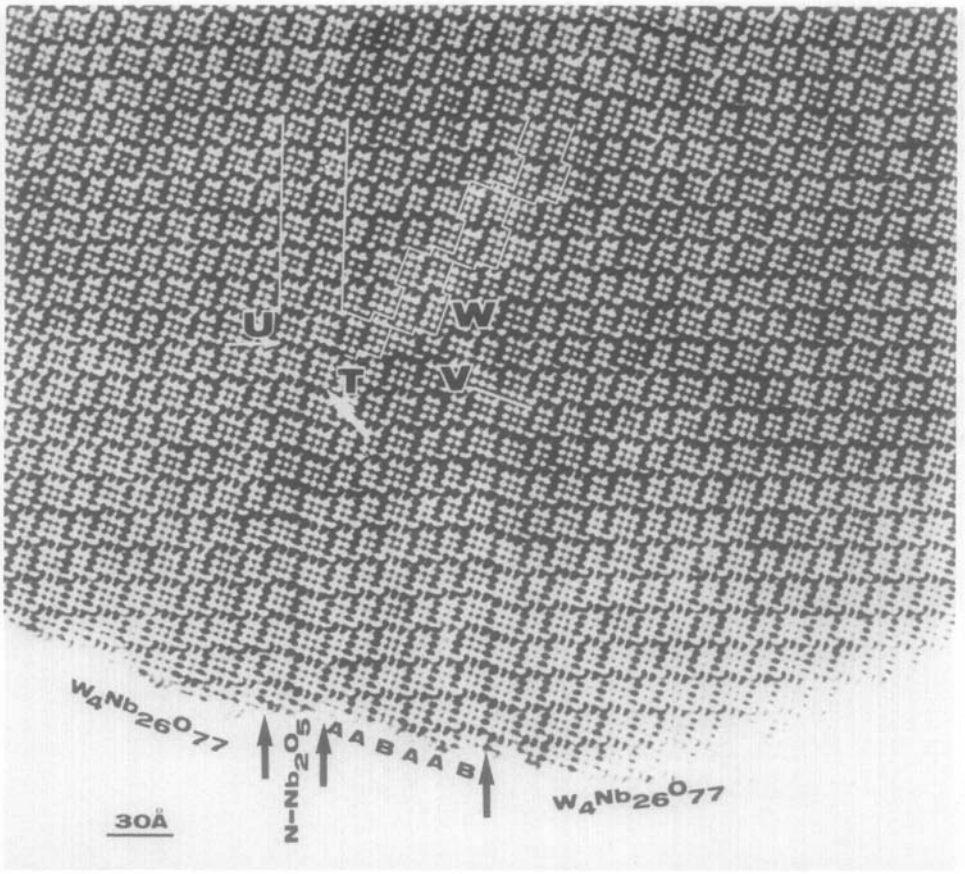

FIG. 4. The [010] structural image of a terminated intergrowth defect containing different kinds of planar defects.

crodomains of $WNb_{12}O_{33}$ and $W_3Nb_{14}O_{44}$ coexisting with $W_4Nb_{26}O_{77}$. Our observation (Fig. 2) now provides the direct evidence of the presence of these two microdomains.

One feature of the structure of $W_4Nb_{26}O_{77}$ is the long-range ordering of two kinds of blocks with different sizes. It is of interest to examine whether other sorts of ordered intergrowth of A and B types of slab can also occur. Some kinds of locally ordered intergrowth structures have indeed been frequently observed. Figure 3 shows one kind of the ordered intergrowth with a sequence of AABAAB . . . slabs. The chemical composition corresponding to this type of structure is $W_5Nb_{38}O_{110}$.

Although in most cases these defects, as mentioned above, traverse the entire field of the crystal fragments, sometimes they are distorted, curved or even terminated inside a crystal as shown in Fig. 4. It is of interest to examine the end structure of the defect in detail to see how they can be accommodated in a perfect ordered structure of $W_4Nb_{26}O_{77}$. A careful study of Fig. 4 shows that two isolated rows of N–Nb_2O_5 and six rows of AABAAB occur in the border region of the crystal in Fig. 4. Both the structures of N–Nb_2O_5 and $W_3Nb_{14}O_{44}$ are

consisting of the same (4 × 4) octahedral blocks but they join differently in these two structures. At T, these two rows of N–Nb_2O_5 are changing into $W_3Nb_{14}O_{44}$ through a (5 × 4) octahedral block. At W, groups of four (5 × 3) octahedral blocks, having a $Nb_{31}O_{77}F$ type of structure, can be seen, where the crystallographic shear planes in $W_4Nb_{26}O_{77}$ are displaced and the structures of N–Nb_2O_5 and AABAAB are changed into the perfectly ordered structure of $W_4Nb_{26}O_{77}$. At V, several (4 × 3) blocks are rotated by 90 degrees in orientation with respect to those in the perfect $W_4Nb_{26}O_{77}$. These show clearly the flexibility of this kind of octahedral structure by changing the size of octahedron blocks, their orientations, and the ways of joining to accommodate any local defects.

References

1. M. SUNDBERG, *Chem. Commun. Univ. Stockholm* No. 5 (1981).
2. S. IIJIMA, *Acta Crystallogr. Sect. A* **29,** 18 (1973).
3. S. IIJIMA AND J. G. ALLPRESS, *J. Solid State Chem.* **7,** 94 (1973).
4. J. L. HUTCHISON, F. J. LINCOLN, AND J. S. ANDERSON, *J. Solid State Chem.* **10,** 312 (1974).
5. J. O. BOVIN, D. X. LI, L. STENBERG, AND H. ANNEHED, "Proceedings, 10th International Congress on Electron Microscopy, Hamburg," Vol. 3, p. 55 (1982).
6. L. KIHLBORG, *Chem. Scr.* **14,** 187 (1978–79).
7. T. EKSTRÖM, AND R. J. D. TILLEY, *Chem. Scr.* **16,** 1 (1980).
8. K. ISHIZUKA, *Acta Crystallogr. Sect. A* **38,** 773 (1982).
9. S. ANDERSSON, W. G. MUMME, AND A. D. WADSLEY, *Acta Crystallogr.* **21,** 802 (1966).
10. J. G. ALLPRESS, J. V. SANDERS, AND A. D. WADSLEY, *Acta Crystallogr. Sect. B* **25,** 1156 (1969).